Removal of Some Cationic Contaminants from Aqueous Solutions Using Sodium Dodecyl Sulfate-Modified Coal Tailings

***Boveiri Shami, Rahim; Shojaei, Vahideh; Khoshdast, Hamid* *+**

Department of Mining Engineering, Higher Education Complex of Zarand, Zarand, I.R. IRAN

ABSTRACT: *A sample coal tailings activated by Sodium Dodecyl Sulfate (SDS) surfactant was used as an efficient adsorbent for the removal of lead from an aqueous solution. The effects of three factors, namely, initial solution pH (3-11), absorbent to lead ratio (12.5-162.5), and contact time (3-31 h), on lead removal, were studied and optimized using response surface methodology. Statistical analyses showed that all factors significantly affect lead removal. Process optimization resulted in maximum lead removal of 99.64% at initial solution pH of 6.75, absorbent to metal ratio of 91.33 and 20 h equilibrium contact time, and 97.4% removal after about 40 min. Kinetic studies revealed that lead adsorption follows the first-order model with a rate constant of 10.39 h^{-1}. The selectivity study in bimetal aqueous systems using copper, lead and zinc metals showed the adsorption order of $Cu^{2+} > Pb^{2+}$, $Pb^{2+} > Zn^{2+}$, and $Zn^{2+} > Cu^{2+}$ with some unusual trends. The lead adsorption on activated coal tailings was also found to follows the Freundlich isotherm model. The interaction mechanisms between SDS and the surface of coal tailings particles were also discussed. This study demonstrates that SDS-activated coal tailings could be considered as a promising efficient, low-cost, and easily available adsorbent for the treatment of heavy metal polluted wastewaters.*

KEYWORDS: *Coal tailings; Sodium dodecyl sulfate; Heavy metal; Adsorption; Kinetics; Selectivity study.*

INTRODUCTION

There are hundreds of coal washing plants around the world that produces and disposes of millions of tons of coal tailings in tailing dams and dumping sites. These rejected coal products face the environment with various health hazards due to their contained heavy metal, sulfur and fines, and possibly, nano-minerals. Contamination of surface and underground sources of water and dispersion of coal dust by wind are two common reasons by which natural ecology can be disturbed [1-4].

Despite numerous environmental hazards, these materials can be considered as a potential and low-cost mineral resources for various uses. According to statistics provided in some technical reports, over 5 billion tons of coal tailings are discarded by coal processing plants every year. These are mainly fines and reject from wash plants, and end up in tailings dams where they are dried and eventually buried. These coal tailings are sold at very low prices, between 2 and 5 USD/ton depending on the content

** To whom correspondence should be addressed.*
+ E-mail: khoshdast_hamid@yahoo.com
1021-9986/2021/4/1105-1120 16/$/6.06

of the coal, which usually varies between 20 and 40 percent; however, due to limited use and commercial customers, a significant portion of it is disposed of intact in the dam [5-9]. Hence, in the case of the development of efficient methods for recycling these materials, they would be of high added value. So far, there have been many attempts, either scientifically or experimentally, to reuse coal tailings. Reasons limiting such efforts may include high moisture content, large mineral-petrographic variation, fragmentation, and low energy characteristics [10]. Generally, methods developed for the recycling of coal tailings can be summarized as follows:

● Recovery of a combustible portion of coal tailings as low energy material for power plants and smelts: Some small companies, for example, produce low energy briquette for domestic consumption [11]; however, new technologies such as nature medium cyclone has aided the efficiency of such processes [12].

● Production of liquid fuels in the form of slurry: Such new fuels are shown to be efficient solutions for the recycling of coal tailings by some researchers. Coal-water slurry can be produced without any further additives [13] or in combination with different oils to improve their ignition characteristics [14].

● In agricultural applications as moisture preservative, soil modifier and fertilizer [15];

● Bio-production of gaseous fuels: *Opara et al.* [16], for example, investigated the production of bio-methane from coal wastes and suggested that these materials can be used as a commercially viable source for the production of methane fuel. Recently, *Zheng et al*. [17] used a microbial consortium derived from sewage sludge for the production of methane from a sample coal waste and showed that coal waste can be partially digested to bio-methane.

● In road construction as foundation materials, railway embankment and asphalt [18-20];

● Manufacture of construction materials such as cement [16], brick [22, 23] and concrete [24].

Today, a variety of methods have been developed to remove pollutants from aquatic environments. Among the various methods, absorption methods have attracted more attention than other methods due to the more well-known mechanism and variety of adsorbents, whose knowledge and technology of production is significantly increasing. In this regard, various absorbents have been studied so far, among which are various types of natural and synthetic zeolites [25-28], nanomaterials [29-36], and low-cost absorbents produced from agricultural wastes [37-41]. One of the new approaches in the production of adsorbents is a variety of composites that are produced by combining conventional adsorbents with each other or with a variety of polymers and surfactants [42-46]. The purpose of producing composites is to increase the adsorption capacity of the adsorbent, which is achieved by increasing the surface charge, specific adsorption surface, or both.

Sodium Dodecyl Sulfate (SDS) is a heteropolar surface active agent with a hydrophobic hydrocarbon chain and a polar head neutralized with the sodium ion. The high solubility and negative character of SDS have led to its widespread use in the detergent industry and the treatment of wastewater to remove contaminants. Sodium dodecyl sulfate can be used in various forms for heavy metal removal from aqueous solutions. Before Critical Micelle Concentration (CMC), SDS can collect heavy metal cations as a free solute anionic collector [47-51], and over CMC, SDS micelles can trap metal cations in the solution [52-55]. Sodium dodecyl sulfate can also interact with non-polar surfaces with the hydrocarbon chain through the physical forces and/or with polar surfaces with chemical bonding *via* its polar head. Therefore, SDS has been considered as an efficient surface modifier for the activation of different types of materials to improve their adsorption capacity. For example, the adsorption capacity enhancement of carbon material coated by SDS has been investigated by some researchers. The hydrocarbon chains of SDS can physically adsorb on the hydrophobic carbon surface *via* van der Waals bonding [56]. For example, it is shown that modification of activated carbon type absorbents with SDS can increase the adsorption of positively charged molecules such as methylene blue dye [57, 58] and heavy metals [59]. On the other hand, the polar head of SDS can chemically interact with special species at the surface of mineral particles and increase their adsorption capacity. Various researchers have used this phenomenon for surface modification of minerals [60-62] and inorganic nanoparticles [62-65].

As mentioned earlier, coal tailings are abundant mining waste that can be employed as an inexpensive and available absorber to remove environmental pollutants. Therefore, the aim of the present study is to present a potential solution to recycling coal wastes by applying the coating effect of sodium dodecyl sulfate

to activate coal tailings as an efficient absorbent for removal of heavy metals from aqueous solutions. Moreover, the main and interaction effects of parameters influencing the removal efficiency, including initial solution pH, absorbent to metal ratio, and contact time were investigated using a systematic experimental design. The process was then modeled and optimized. Adsorption selectivity, kinetics, and mechanism were also evaluated.

EXPERIMENTAL SECTION

Coal tailings sample and reagents

The studied coal tailing was carefully sampled from the tailings dam of Zarand Coal Washing Plant (Zarand, Iran). Particle size analysis revealed that 95% by weight of tailings sample is smaller than 100 μm with 72% ash content as indicated by ash analysis performed according to ASTM D 3174-73 Standard. Chemical analysis was conducted using X-Ray Fluorescence (XRF, Rigaku, NEX DE) spectrometer. Scanning electron microscopy (SEM, Tescan, Vega-II microscope) was also used to investigate the surface status of coal tailings before and after modification. Sodium Dodecyl Sulfate (SDS) reagent (with over 99% purity) was obtained from Merck. Metal salts including $Pb(NO_3)_2$, $Zn(NO_3)_2{\cdot}6H_2O$, and $Cu(NO_3)_2{\cdot}2.5H_2O$, and pH regulators including HCl and NaOH were also obtained from Merck and used with no further purification.

Adsorption variables and experimental design

Different experimental designs are developed for the evaluation of the effect of operating variables on a process response. In this study, a Central Composite experimental Design (CCD) was used to evaluate the effects of some parameters, that frequently considered by many investigators, i.e. the initial solution pH, absorbent to metal (C/M) ratio, and contact time on lead removal from a synthetic aqueous environment as process response. Using the central composite design, both main effects, either linear or non-linear, and interaction effects can be recognized. In addition, CCDs are very powerful designs for process optimization and identification of optimum conditions under which maximum process efficiency can be obtained. The levels of variables studied are given in Table S1. The final experimental design used for adsorption tests is shown in Table 1.

Adsorption experiments and analyses

In order to activate the coal tailings, 50 g of sample was first washed with distilled water, dried at 60°C, and added to 200 mL of concentrated SDS solution. The mixture was then left for 24 h on a magnetic stirrer set at 150 rpm. Afterward, the mixture was filtered, dried at 60°C, and kept in a cool and dry place for further use. For each batch adsorption experiment, 250 mL of an initial solution containing 100 ppm of lead ion and requisite amounts of activated coal waste was prepared at room temperature (about 26±1°C). After pH adjustment using 0.1 M HCl and 0.1 M NaOH, the solution was stirred with a magnetic stirrer at 200 rpm. After the desired contact time, the flasks were withdrawn from the magnetic stirrer and the mixture was filtered and the residual solution was analyzed for metal content. Selectivity studies were carried out in presence of Cu and Zn metals. The bimetal competitive adsorption tests were conducted using a solution containing an equal concentration of both metals. All other factors were kept constant under optimum conditions. At the end of each test, the solution was filtered and analyzed for metal content. Then, the selectivity coefficients were calculated by plotting selectivity curves. The process kinetics was investigated by a periodical sampling of solution during the optimum test. The adsorption models were also studied for metal solutions with different initial concentrations.

The metal content of the samples taken from the bulk solution was measured by an atomic absorption instrument (Varian model SperctAA 220, Mulgrave, Victoria). The removal efficiency of adsorption was calculated by:

$$\text{Removal},\% = \frac{(C_0 - C_e)}{C_0} \times 100 \quad (1)$$

where C_0 is the initial concentration of metal in the solution and C_e represents the final metal concentration at equilibrium time

RESULTS AND DISCUSSION

Sample characterization results

The chemical analysis using XRF showed that the ash portion mostly includes Si and Al oxides (Table 2). The SEM image of tailings sample before and after modification by SDS is shown in Fig. 1. As seen, the tailings sample includes angular particles with no unusual surface pattern and excess void spaces. In presence of SDS, however, particles are attached to one another so that agglomerates are formed.

Table 1: Central composite design consisted of experiments for the study of operating parameters with experimental results.

Run	A: pH	B: C/M Ratio	C: Time	Pb Removal (%)
1	7	87.5	17	99.22
2	5	50	10	47.50
3	5	50	24	100
4	3	87.5	17	60.50
5	9	125	24	99.63
6	9	50	24	100
7	5	125	24	99.43
8	7	87.5	17	96.75
9	9	125	24	99.42
10	9	50	10	99.11
11	5	50	10	56.40
12	7	87.5	17	75.01
13	5	125	10	87.56
14	9	125	10	98.33
15	7	87.5	3	87.30
16	7	87.5	17	96.46
17	7	12.5	17	38.90
18	9	125	10	96.90
19	5	125	24	98.63
20	9	50	10	97.82
21	7	87.5	31	98.29
22	5	125	10	98.42
23	7	87.5	17	98.91
24	11	87.5	17	97.82
25	9	50	24	99.67
26	7	162.5	17	99.47
27	7	87.5	17	99.32
28	5	50	24	77.75

Table 2: Chemical analysis of the studied coal tailings sample.

Component	SiO_2	Al_2O_3	CaO	Fe_2O_3	K_2O	SO_3	Rest*
Portion (%)	49.1	25.8	5.5	5.9	5.6	4.0	4.1

**P_2O_5, TiO_2, MnO, MgO, Na_2O, L.O.I*

Analysis of variance (ANOVA) of results

Generally, central composite design applies a nonlinear multi-variable regression equation to model the relation between process response and operating variables. The CCD model includes three sets of coefficients, i.e. constant, linear and nonlinear, which are estimated by statistical approaches. In this study, Design Expert v.7 (DX7) software was used for the calculation of

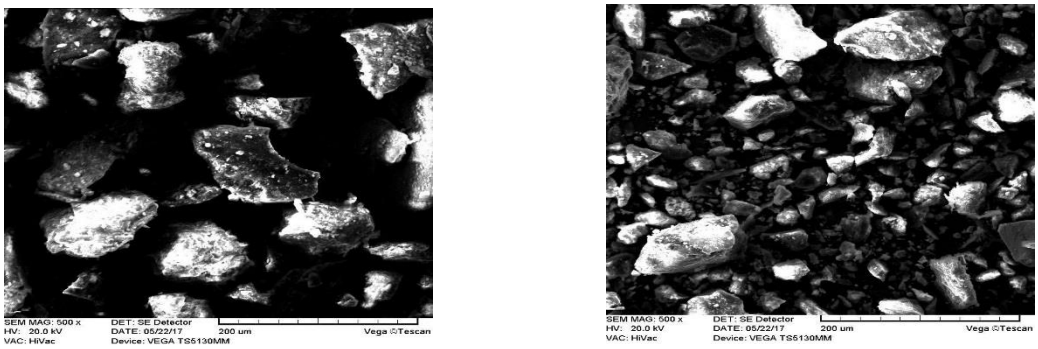

(a) (b)

Fig. 1: SEM images of the coal tailings particles (a) before and (b) after modification by SDS.

the prediction model. The best-fitted model equation was obtained for Pb removal as follows:

$$\text{Lead removal (\%)} = 99 + 10.51A + 10.64B + 3.34C - 8.68AB - 2.82AC - 1.66BC - 3.28A^2 - 6.91B^2 - 1.01C^2 \quad (2)$$

where factors are in coded form. Model Eq. (2) was used to evaluate the influence of the process variables on Pb removal. The significance of the model is evaluated by analysis of variance (ANOVA). Table S2 shows the ANOVA results. A confidence interval of 95% was chosen for the determination of the significance of main and interaction effects. As shown in Table S2, the suggested regression model is significant due to the value of Fisher's *F*-test (F model = 22.62) with a very low probability value (*p* model < 0.0001). Table S2 also indicates that the effects of all variables are significant (p values less than 0.05). The effect between pH and absorbent to Pb ratio (AB) is the sole significant interaction effect. Although the other interaction effects are not significant, they had sharp effects on the model accuracy. The normal probability of the residuals for Pb removal, shown in Fig. 2, indicates that almost no serious violation of the assumptions underlying the analyses, which confirmed normality assumptions and independence of the residuals. In addition, closely high values of the model correlation coefficient (R^2 = 93.14%) and adjusted correlation coefficient (Adj R^2 = 89.02%) also showed the high significance of the model. The Adeq precision shows the signal-to-noise ratio; a ratio of greater than 4 is a desirable value [66]. In this investigation, the ratio was 13.54, which indicated an adequate signal. Thus, the model could be used to navigate the design space.

Effect of solution pH

The variation of lead removal at various initial solution pH values is shown in Fig. 3. As can be seen, the Pb removal efficiency increases as the solution pH increases. The pH value of the medium has a critical role in the entire adsorption process as well as in the adsorption capacity of the coal tailings. As will be discussed later, the lead adsorption on the surface of SDS-activated coal tailings follows the multilayer mechanism with non-uniform distribution of adsorption energy on the surface of tailings particles. Therefore, it can be stated that the adsorption of lead cations is partially due to the interaction with SDS anions on the surface of tailings particles and partially due to the interaction with negatively charged points on the tailings particles surface which is not covered by SDS molecules. As solution pH increases up to about 7 at which SDS represents maximum surface activity, lead adsorption increases; afterward, the interaction between lead cations and SDS molecules decreases due to the increase of Na^+ concentration and the decrease of SDS activity. Similar results were also observed by other researchers. By increasing the pH, negatively charged functional groups of SDS molecules may be scattered on the surface of coal tailings particles and entailed an increase in the electrostatic gravity between the adsorbent surface and the cations and an augment in adsorption. They are separated on the surface of the adsorbent, and the negative charge surface results in an increase in the electrostatic gravity between the adsorbent surface and the cations as well as an increase in adsorption [37]. It is shown that the point of zero charge (PZC) of coal materials varies in the pH range of 4-6 depending on the ash content

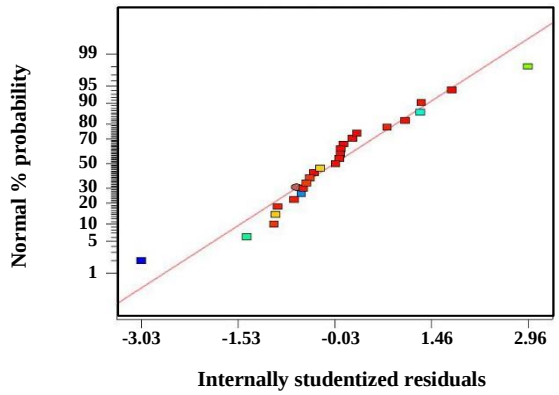

Fig. 2: Normal plot of the residuals for lead removal model.

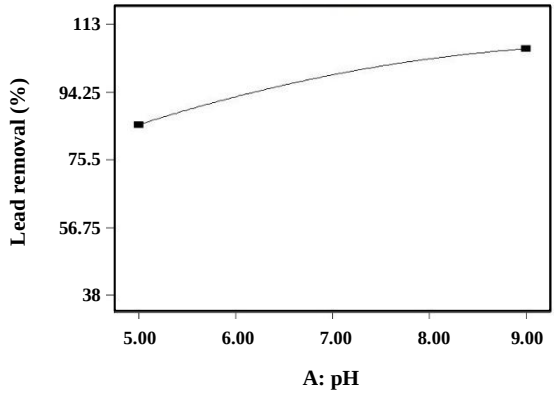

Fig. 3: Effect of initial solution pH on lead removal.

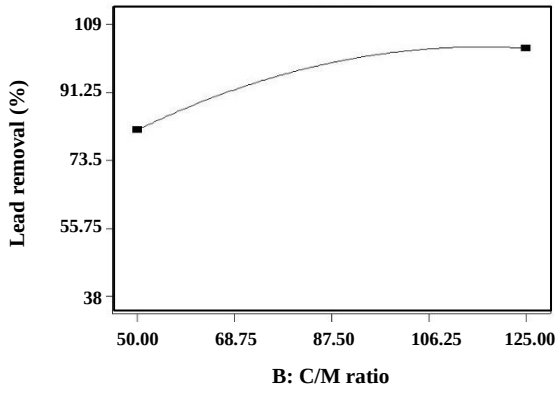

Fig. 4: Effect of absorbent to metal ratio on lead removal.

of coal sample [67, 68]. At pH values higher than PZC, the surface of coal particles become negatively charged; therefore, the increase of lead adsorption at alkaline pH can be attributed to the higher active points of coal tailings particles which consequently increases the adsorption of the Pb cations through electrostatic forces of attraction and provides multilayer adsorption.

Effect of adsorbent dose

The effect of adsorbent dose on lead removal is represented in Fig. 4. It is clear that Pb removal increases as the absorbent dose is increased because the number of adsorption sites increases, and consequently, more Pb species adsorb on the activated coal tailings particles. However, the removal reaches a maximum value at an absorbent to lead ratio of around 100 and after that follows a linear trend. This implies that adsorption sites at this absorbent to lead ratio may be enough to completely treat 250 mL of 100 ppm lead solution. This is due to certain initial factors, including the occupancy of almost all active sites of adsorption using lead ions, and the created balance between the metallic ions absorbed on the surface of tailings particles and the remaining cations in the solution [31, 37].

Effect of contact time

The effect of contact time on lead removal is shown in Fig. 5. It shows that Pb removal follows a slightly increasing trend with time; Fig. 5 also shows that Pb adsorption on coal tailings is fast in the initial stage of the adsorption process. Referring to Table S1, it is observed that even at a very short time considered in lower extrapolation level, i.e. 3 h in run 15, over 87% Pb is sequestered from the solution. In the early stages of the process that the adsorption sites of adsorbent are vacant, adsorption of lead initiates with a faster rate as a result of the diffusion process from the bulk solution to the adsorption sites. Afterward, the adsorption rate gradually decreases as the contact time elapses to the equilibrium state due to the saturation of the active sites [69]. Fig. 6 shows the incremental variation of Pb removal over optimum adsorption time. As seen, the rate of Pb adsorption increases up to 40 min, and then, approaches a nearly linear trend. This is because of the large number of vacant surface areas available for molecule absorption during the early stages of absorption; however, occupied areas begin to excrete absorbing molecules in the soluble phase at terminal times. In the case of molecule absorption, the available stimulatory forces are weakened to reach the empty surface areas, hence the reduction in adsorption [37]. Thus, to ensure the state of equilibrium for Pb adsorption,

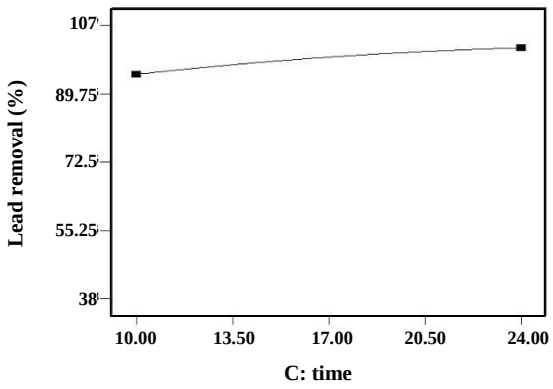

Fig. 5: Effect of contact time on lead removal.

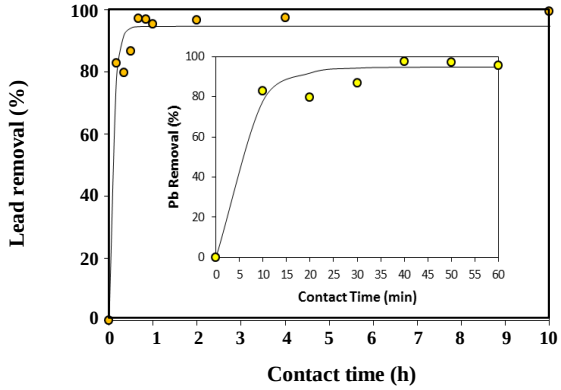

Fig. 6: Classic first-order kinetics plot for the removal of lead from aqueous solution.

60 min was considered as the equilibrium time for further studies.

Analysis of interaction effects

The three-dimensional (3D) response plots of the model response vs. two independent variables varying within their experimental levels while maintaining other variables at their mid-levels can give useful information on their relationships [70]. Therefore, in order to gain a better understanding of the individual effects of the studied operating variables and their corresponding interaction effects on the other variables, 3D response plots for the lead removal was constructed based on the nonlinear model proposed by DX7 software. Since the model in this study had three independent variables, one variable was held constant at its mid-level for each plot. The 3D surface plots for studied variables are visualized in Fig. 7. As seen in Fig. 7, all interactions show non-linear effects on response. Fig. 7 reveals that maximum Pb removal can be obtained for pH and absorbent to lead ratio at their middle levels and for contact time at around its low level.

Process optimization

Design-Expert is a powerful tool for the prediction of optimal conditions under which maximum response value would be obtained. The software uses the prediction model developed on the basis of statistical analysis and then, presents a list of optimal conditions with their corresponding response values. After setting the value limits for all model parameters, DX7 presented 7 optimal conditions sets with maximum lead removal of 100% (Table 3). The first point with moderate conditions was chosen as the optimum test and replicated three times to ensure its accuracy. Therefore, maximum Pb removal of 99.64% can be obtained at pH 6.75 and absorbent to lead ratio of 91.33 after 20 h adsorption.

Selectivity studies

Selectivity in mixed-metal solutions is also important in the adsorption process. For example, the target metal might not be removed from a solution that contains a large excess of other metallic ions that compete with the target metal in the electrical attraction for available absorbent binding sites. This problem can be overcome by selective complexation between a specific surfactant and the target metal. The complex itself could then function as a surfactant. It could also provide a clue to the metal's recovery. The selectivity of metal adsorption by activated coal tailings was calculated as follows [71]:

$$\ln C_A = S_B^A \ln C_B + c \quad (3)$$

Where S_B^A is the selectivity coefficient of metal *A* over metal *B*, C_A and C_B are the concentrations of counterions *A* and *B*, and *c* is constant. The adsorption selectivity by SDS-activated coal tailings was assessed by the measurement of the selectivity coefficients for all bimetal aqueous systems. Fig. 8 shows the competitive adsorption between different bimetal systems. The selectivity coefficients and equilibrium metal removals for competitive systems are listed in Table 4. Referring to Fig. 8 and Table 4, it is observed that more selective metal in each bimetal system yields higher adsorption removal. In Cu–Pb system,

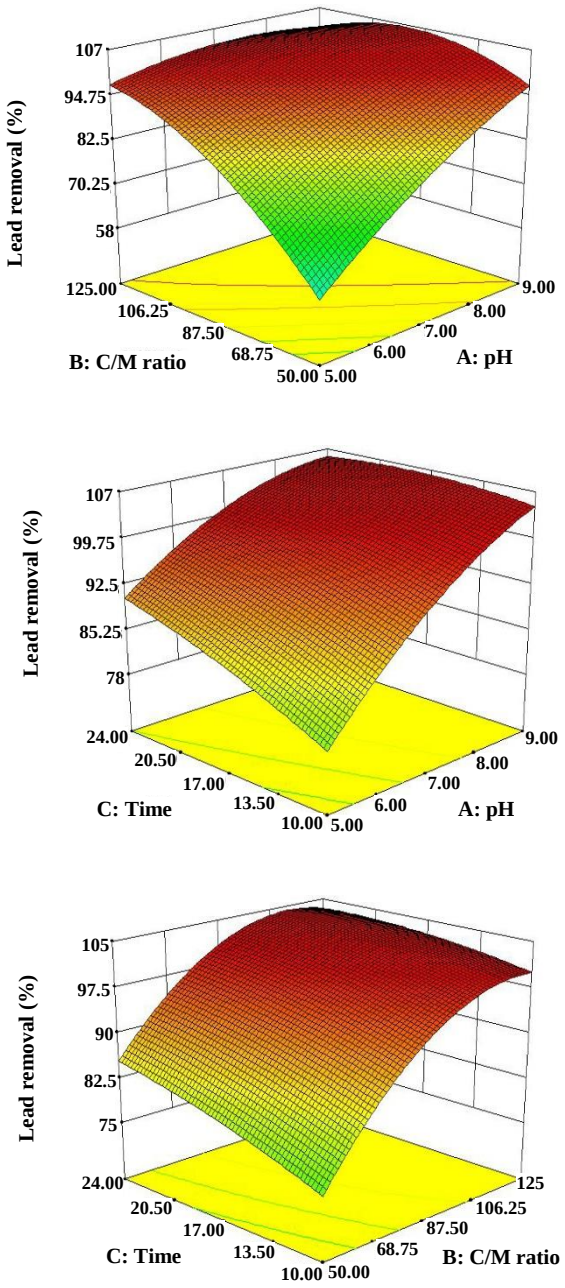

Fig. 7: The 3D response plots showing the interaction effects of operating variables on lead removal.

selectivity coefficient of about unit indicates that both Cu and Pb cations show relatively equal tendency to adsorb on activated tailings particles. Close values of maximum removal for both metals also confirm their relatively equal adsorption tendency. In Pb–Zn system, lead shows much higher removal than zinc, and thus, a higher selectivity coefficient could be expected. Given the selectivity orders of Cu–Pb and Pb–Zn systems, i.e. Cu > Pb and Pb > Zn, copper is expected to be more selective than zinc but experimental investigation showed a different result. Therefore, representing a tidy selectivity order for three metals is difficult. In addition, as seen in Fig. 8, the adsorption removals for Cu–Pb and Pb–Zn systems vary inversely with a slight difference after around 30 min of contact time. Such an unusual trend can be attributed to a number of likely phenomena as below:

- There may happen potential competitive multilayer adsorption due to electrostatic interaction between the electron could of the first monolayer adsorbed on the surface of the modified coal particles and the second layer of metal ions; or
- There may be some free adsorption zones between individual metal ions adsorbed on the surface of the coal particles where can be later occupied by those secondary metal ions adsorbed on the surface.

Further studies are required to interpret these unusual observations.

Adsorption kinetics

The kinetics of lead adsorption on activated coal tailings was preliminarily determined using Lagergren's pseudo-first-order (Eq. (3)) and Ho's pseudo-second-order model (Eq. (4)), as follows [72]:

$$\ln\left(1-\frac{q_t}{q_e}\right) = -k_1 t \tag{4}$$

$$\frac{1}{q_t} - \frac{1}{q_e} = \frac{1}{k_2 q_e^2 t} \tag{5}$$

Where k_1 is the rate constant of pseudo-first-order adsorption (h^{-1}), q_e (mg/g) is the amount of solute adsorbed on the surface at equilibrium, and k_2 is the equilibrium rate constant of pseudo-second-order sorption (g/mg h), and q_t (mg/g) is the amount of solute adsorbed at any time t:

$$q_t = \frac{(C_0 - C_t)V}{W} \tag{6}$$

Where C_0 is the initial concentration of Pb (mg/L), C_t is the liquid-phase concentration of Pb at time t (mg/L), W is the mass of adsorbent used (g) and V is the volume of the solution (L). The comparison of the adsorption kinetics data for pseudo-first-order and pseudo-second-order models of lead adsorption on activated coal tailings is shown in Fig. S1(a), (b). As seen in Fig. S1, lead adsorption does not show reliable fitting accuracy to any

Table 3: Optimal conditions suggested by DX7 to achieve maximum lead removal.

Set no.	pH	C/M Ratio	Time	Predicted Removal (%)
1	6.75	91.33	19.70	100
2	9	50	24	100
3	8.26	107.88	23.73	100
4	7.63	108.58	17.79	100
5	8.5	105.47	23.42	100
6	5	125	24	100
7	6.73	120.25	18	100

Table 4: Selectivity coefficients and orders for different bimetal aqueous systems.

Bimetal System	R_H (%)	R_L (%)	Selectivity Coefficient	Selectivity Order
Cu–Pb	Cu, 29.90	Pb, 27.70	1.08	Cu > Pb
Pb–Zn	Pb, 81.40	Zn, 29.20	1.37	Pb > Zn
Zn–Cu	Zn, 26.8	Cu, 21	1.13	Zn > Cu

of the models. In order to determine the kinetics of lead adsorption, the conventional first-order exponential model was also evaluated with experimental data. The conventional first-order equation is in the following form:

$$R = R_{\infty}(1 - e^{-kt}) \quad (7)$$

where R and R_∞ are the incremental and maximum removals (%), respectively and k is the kinetic constant rate (h^{-1}). As shown in Fig. 9, lead adsorption is well fitted with the first-order model with a high correlation coefficient of 96.65%. The first-order rate constant was found to be 10.39 h^{-1} which is in agreement with time effect interpretation, i.e. fast adsorption in initial contact times.

Adsorption isotherms

The equilibrium isotherm plots are useful tools for indicating the relation between the amounts of metal removed from aqueous solutions at equilibrium state by a mass unit of adsorbent at a constant temperature. Various isotherm plots are developed that between them, the Langmuir, Freundlich, Temkin, and Jovanovic isotherm models are widely used in absorption investigations. Each model describes how the adsorbate interacts with the surface of the absorbent. The Langmuir isotherm indicates the monolayer adsorption of metal onto a homogenous surface containing a finite number of identical sites by assuming that adsorption energies uniformLy distribute onto the surface. The Langmuir isotherm and the linear form of this model are represented in Eqs. (8) and (9), respectively [73-75]:

$$q_e = \frac{q_m K_L C_e}{1 + K_L C_e} \quad (8)$$

$$\frac{q_e}{C_e} = \left(\frac{1}{K_L q_m}\right) + \left(\frac{C_e}{q_m}\right) \quad (9)$$

The Freundlich isotherm indicates the potential multilayer adsorption of adsorbate species onto a heterogeneous surface with a non-uniform distribution of adsorption energies over the surface of the absorbent. The Freundlich isotherm and the linear expression of this equation are in the form of Eqs. (10) and (11), respectively [76]:

$$q_e = K_L C_e^{1/n} \quad (10)$$

$$\ln q_e = \ln K_F + \frac{1}{n}\ln C_e \quad (11)$$

The Temkin model considers that the adsorption heat of all molecules in the layer would decrease linearly with coverage and is characterized by a uniform distribution of binding energies up to some maximum binding energy. The normal and linearized forms of Temkin isotherm model are as follows, respectively [75]:

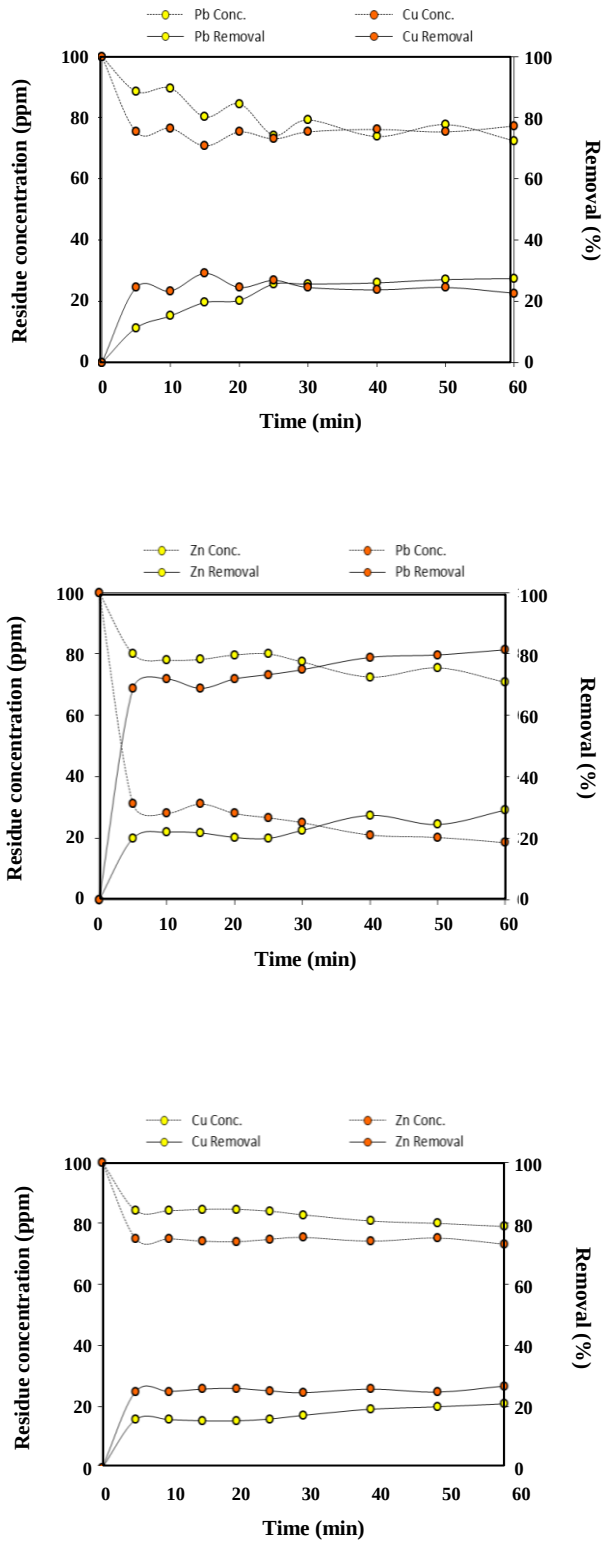

Fig. 8: The residual concentrations and removals of metals in competitive systems.

$$q_e == q_m \ln(K_T C_e) \quad (12)$$

$$q_e = q_m \ln K_T + q_m \ln C_e \quad (13)$$

The Jovanoic isotherm is based on the same assumptions of the Langmuir isotherm; in addition, this model also considers the possibility of some mechanical contacts between the adsorbing and desorbing molecules on the homogeneous surface. The Jovanoic isotherm and its linear expression are represented in Eqs. (14) and (15), respectively [69]:

$$q_e == q_m \exp(K_J C_e) \quad (14)$$

$$\ln q_e = \ln q_m + K_J C_e \quad (15)$$

The experimental data were compared to the Langmuir, Freundlich, Temkin, and Jovanovic equilibrium equations. The corresponding plots for these isotherm models are shown in Fig. S2. The applicability of each isotherm to describe the adsorption process was identified by the correlation coefficients (R^2 values). Average Relative Error (ARE) between experimental and calculated equilibrium metal concentration absorbed on the absorbent surface (q_e) was also calculated by means of Eq. (16):

$$ARE = \frac{100}{N} \sum_{i=1}^{N} \left| \frac{q_{e,exp} - q_{e,cal}}{q_{e,exp}} \right| \quad (16)$$

where $q_{e,exp,}$ and $q_{e,cal}$ are experimental and calculated lead concentration at equilibrium state, respectively, and N is the number of experiments. Commonly, lower ARE beside high R^2 values can be a good criterion for choosing the best-fit model. The values of isotherm parameters, correlation coefficients, and ARE values are listed in Table 5. As seen in Table 5, the Freundlich isotherm model shows better fitting accuracy than other isotherm models because of the higher correlation coefficient and lower ARE. Both the correlation coefficients and ARE values for a linearized form of Langmuir, Temkin, and Jovanovic models are low therefore describing experimental data. these isotherms cannot be good models for

Adsorption mechanisms

Coal tailings include three different types of particles: completely liberated ash particles, completely liberated coal particles, and interlocked ash-coal particles (middlings). Therefore, various mechanisms may involve in the coal tailings activation by sodium dodecyl sulfate

Table 5: Isotherms parameters, correlation coefficients value and ARE for lead adsorption.

Isotherm	Model Parameters		Correlation Coefficient (R^2, %)	Relative Error (ARE, %)
Langmuir	q_m = 78.740	K_L = 0.042	77.86	20.66
Freundlich	K_F = 8.517	n = 2.285	95.54	9.67
Temkin	q_m = 11.016	K_T = 1.240	71.64	35.39
Jovanoic	q_m = 14.065	K_T = 0.027	82.29	275.55

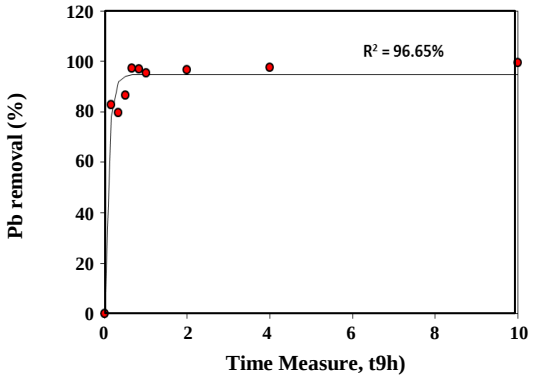

Fig. 9: Fitting plots for conventional first-order model of lead adsorption.

and thus, heavy metal adsorption on the surface of tailings particles. The suggested mechanisms can be summarized as schematically illustrated in Fig. 10 as follows:

● As an anionic surfactant, negatively charged polar heads of SDS can interact with active points on the surface of those ash particles which have taken positive charge due to the presence of cations such as Al^{3+}, $Ca^{2+,}$ etc. (Fig. 10a). In this case, SDS molecules adsorb on the surface such that hydrocarbon chains orient into the aqueous environment. Afterward, the second layer of SDS molecules connect to the first layer via van der Waals bonding and leave their polar heads to the solution. These anionic heads can then adsorb heavy metal cations from the solution (Fig. 10a.1). At concentrations beyond the CMC, SDS molecules may adsorb at the surface of ash particles in the form of the micelle (Fig. 10a.2). At this condition, more anionic functions are available for interacting with heavy metal ions. However, some SDS molecules may individually absorb on the surface of the ash particles and therefore, cannot interact with metal ions (Fig. 10a.3).

● If ash particles are negatively charged due to the higher activity of oxygen ions, especially at alkaline pH values, SDS molecules cannot adsorb on the surface due to the repulsive forces. Thus, heavy metal cations would directly react with anionic functions on the surface of ash particles (Fig. 10b).

● In the case of naturally non-polar coal particles, SDS adsorption on the surface would be of the physical type with van der Waals bonding between SDS hydrocarbon chains and carbon functions at the surface of coal particles. As a result, SDS molecules orient towards the solution so that anionic heads can adsorb metal cations (Fig. 10c.1). The position of SDS molecules adsorbed on the surface can lead to the formation of various forms of hemi-micelles (Figs. 10c.2 and 10c.3) and consequently, to single or multilayer adsorption of heavy metals.

In the case of middling particles which are the largest portion of coal tailings, various aforesaid mechanisms may be involved (Fig. 10d) and this can be the main reason for the non-uniform distribution of adsorption energy over the surface of activated coal tailings particles.

CONCLUSIONS

The present study reveals that heavy metal polluted wastewaters can efficiently be treated by coal tailings activated by Sodium Dodecyl Sulfate (SDS) surfactant. The effect of activation on the removal of lead, as reference metal, was evaluated using response surface methodology with solution pH, absorbent to metal ratio, and contact time as process variables, and lead removal as process response. Process optimization revealed that maximum lead removal of 99.64% can be achieved at initial solution pH of 6.75 and absorbent to metal ratio of 91.33 in about 20 h of contact time. However, the removal can be reached to 97.4% after about 40 min of adsorption, if less process duration is required. Experiment at optimum conditions using non-activated coal waste only yielded 27.31% lead removal which confirms the effective role of SDS surfactant on tailings activation. Further investigations on kinetics, adsorption mechanism, and selectivity indicated

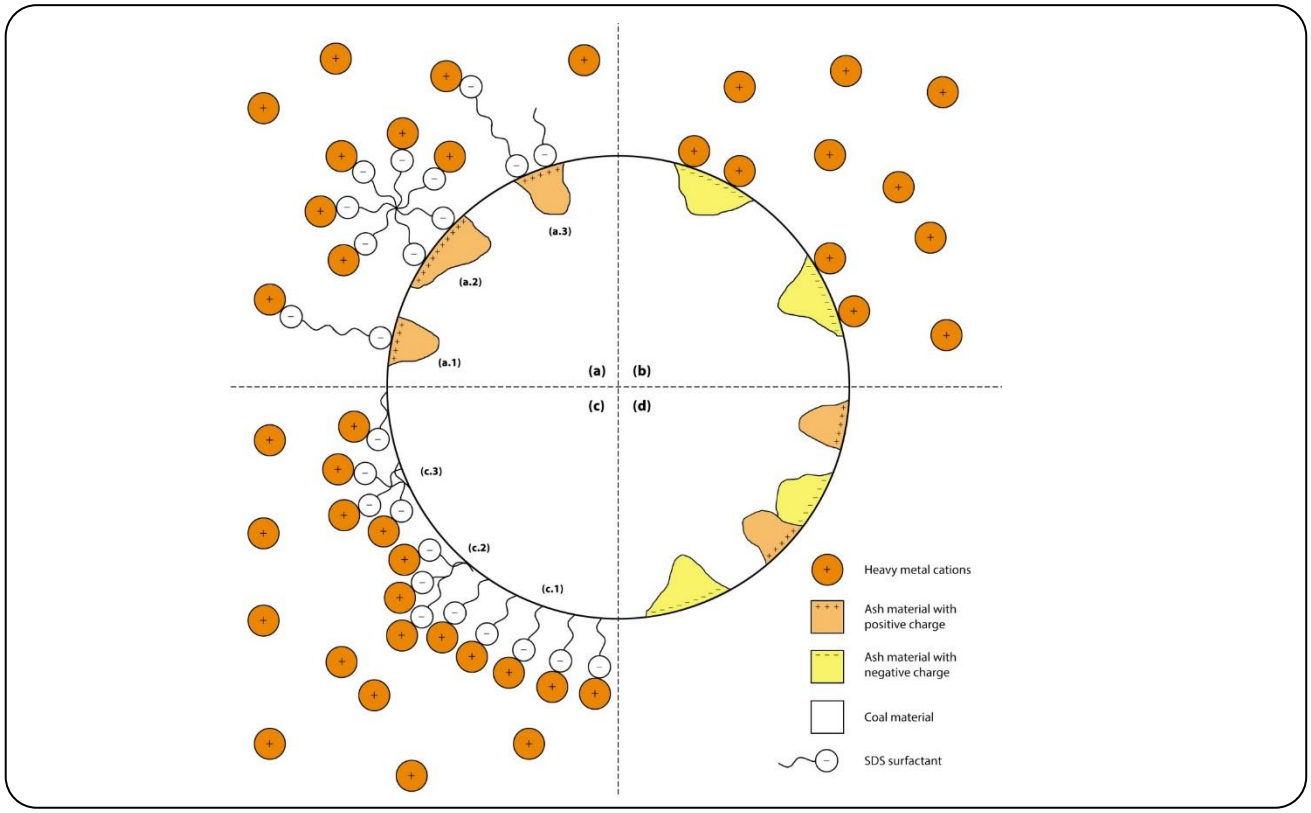

Fig. 10: Suggested mechanisms for heavy metal adsorption on the surface of SDS modified coal tailings particles.

that lead adsorption on coal tailings follows a first-order model with a rate constant of 10.39 h^{-1}. The adsorption modeling showed that the best-fit model is the Freundlich isotherm. The selectivity studies showed some unusual trends in metal selectivity orders. This study showed that coal tailings modified by SDS surfactant can be used as a potentially efficient and low-cost adsorbent for heavy metal removal from wastewaters.

Acknowledgments

Technical supports from FOCUS® Minerals Engineering Research Center (Zarand, Iran) are gratefully acknowledged.

Received : Oct.28, 2019 ; Accepted : Feb.17. 2020

REFERENCES

[1] Mazumder B., "Coal Science and Engineering", Woodhead Publishing, India (2012).

[2] Chudy K., Marszałek H., Kierczak J., Impact of Hard-Coal Waste Dump on Water Quality - A Case Study of Ludwikowice Kłodzkie (Nowa Ruda Coalfield, SW Poland), *Journal of Geochemical Exploration*, **146**: 127−135 (2014).

[3] Civeira M.S., Pinheiro R.N., Gredilla A., Vallejuelo S.F.O., Oliveira M.L.S., Ramos C.G., Taffarel S.R., Kautzmann R.M., Madariaga J.M., Silva L.F.O., The Properties of the Nano-Minerals and Hazardous Elements: Potential Environmental Impacts of Brazilian Coal Waste Fire, *Science of the Total Environment*, **544**: 892−900 (2016).

[4] Lin H., Li G., Dong Y., Li J., Effect of pH on the Release of Heavy Metals from Stone Coal Waste Rocks, *International Journal of Mineral Processing*, **165**: 1−7 (2017).

[5] Committee on Coal Waste Impoundments, "Coal Waste Impoundments: Risks, Responses, and Alternatives", National Academies Press, USA (2002).

[6] National Research Council, "Managing Coal Combustion Residues in Mines", National Academies Press, USA (2006).

[7] Price J.A., Sheafer P.W., Coxe E.B., "Report of Commission Appointed to Investigate the Waste of Coal Mining", Book on Demand Ltd., USA (2013).

[8] Pennsylvania Coal Waste Commission, "Report of Commission Appointed to Investigate the Waste of Coal Mining With the View to the Utilizing of Waste", Sagwan Press, USA (2015).

[9] Wu D., "Mine Waste Management in China: Recent Development", Springer, USA (2020).

[10] Fecko P., Tora B., Coal Waste: Handling, Pollution Impacts and Utilization. In: D. Osborne (Ed.), "The Coal Handbook" (pp. 63−84). Woodhead Publishing Limited, India (2013).

[11] Shen L., Lv W., Zhou W., Zhu J., Qiao E., Recycling Coal from Coal Gangue, *Filtration + Separation*, **54(3)**: 40−41 (2017).

[12] Chu K., Chen J., Yu A.B., Williams R.A., Numerical Studies of Multiphase Flow and Separation Performance of Natural Medium Cyclones for Recovering Waste Coal, *Powder Technology*, **314(1)**: 532−541 (2017).

[13] Dmitrienko M.A., Strizhak, P.A., Environmentally and Economically Efficient Utilization of Coal Processing Waste, *Science of the Total Environment*, **598**: 21−27 (2017).

[14] Vershinina K.Y., Lapin D.A., Lyrschikov S.Y., Shevyrev S.A., Ignition of Coal-Water Fuels Made of Coal Processing Wastes and Different Oils, *Applied Thermal Engineering*, **128**: 235−243 (2018).

[15] Osborne D., "The Coal Handbook", Woodhead Publishing Limited, India (2013).

[16] Opara A., Adams D.J., Free M.L., McLennan J., Hamilton J., Microbial Production of Methane and Carbon Dioxide From Lignite, Bituminous Coal, and Coal Waste Materials, *International Journal of Coal Geology*, **96–97**: 1−8 (2012).

[17] Zheng H., Chen T., Rudolph V., Golding S.D., Biogenic Methane Production from Bowen Basin Coal Waste Materials, *International Journal of Coal Geology*, **169**: 22−27 (2017).

[18] Modarres A., Ayar P., Coal Waste Application in Recycled Asphalt Mixtures with Bitumen Emulsion, *Journal of Cleaner Production*, **83**: 263−272 (2014).

[19] Modarres A., Rahmanzadeh A., Application of Coal Waste Powder as Filler in Hot Mix Asphalt, *Construction and Building Materials*, **66**: 476−483 (2014).

[20] Modarres A., Rahmanzadeh A., Ayar P., Effect of Coal Waste Powder in Hot Mix Asphalt Compared to Conventional Fillers: Mix Mechanical Properties and Environmental Impacts, *Journal of Cleaner Production*, **91**: 262−268 (2015).

[21] Frías M., Sanchez de Rojas M.I., García R., Juan Valdés A., Medina C., Effect of Activated Coal Mining Wastes on the Properties of Blended Cement, *Cement and Concrete Composites*, **34(5)**: 678−683 (2012).

[22] Stolboushkin A.Y., Ivanov A.I., Fomina O.A., Use of Coal-Mining and Processing Wastes in Production of Bricks and Fuel for their Burning, *Procedia Engineering*, **150**: 1496−1502 (2016).

[23] Taha Y., Benzaazoua M., Hakkou R., Mansori M., Coal Mine Wastes Recycling for Coal Recovery and Eco-Friendly Bricks Production, *Minerals Engineering*, **107**: 123−138 (2017).

[24] Wang J., Qin Q., Hu S., Wu K., A Concrete Material with Waste Coal Gangue and Fly Ash Used for FarmLand Drainage in High Groundwater Level Areas, *Journal of Cleaner Production*, **112(P1)**: 631−638 (2016).

[25] Shojaei S., Shojaei, S., Pirkamali M., Application of Box–Behnken Design Approach for Removal of Acid Black 26 from Aqueous Solution Using Zeolite: Modeling, Optimization, and Study of Interactive Variables, *Water Conservation Science and Engineering*, **4(1)**: 13−19 (2019).

[26] Hui K.S., Chao C.Y.H., Kot S.C., Removal of Mixed Heavy Metal Ions in Wastewater By Zeolite 4A and Residual Products from Recycled Coal Fly Ash, *Journal of Hazardous Materials*, **127(1)**:89–101 (2005).

[27] Ioannou Z., Karasavvidis C., Dimirkou A., Antoniadis V., Adsorption of Methylene Blue and Methyl Red Dyes from Aqueous Solutions onto Modified Zeolites, *Water Science and Technology*, **67(5)**: 1129–1136 (2013).

[28] Cheng T., Chen C., Tang R., Han C.H., Tian Y., Competitive Adsorption of Cu, Ni, Pb, and Cd from Aqueous Solution onto Fly Ash-Based Linde F(K) Zeolite, *Iranian Journal of Chemistry and Chemical Engineering*, **37(1)**: 61-72 (2018).

[29] Shojaei S., Shojaei S., Optimization of Process Variables by the Application of Response Surface Methodology for Dye Removal Using Nanoscale Zero-Valent Iron, *International Journal of Environmental Science and Technology*, **16(8)**: 4601–4610 (2019).

[30] Shojaei S., Shojaei S., Sasani M., The Efficiency of Eliminating Direct Red 81 by Zero-Valent Iron Nanoparticles from Aqueous Solutions Using Response Surface Model (RSM), *Modeling Earth Systems and Environment*, **3(1)**: 27 (2017).

[31] Shojaei S., Khammarnia S., Shojaei S., Sasani M., Removal of Reactive Red 198 by Nanoparticle Zero Valent Iron in the Presence of Hydrogen Peroxide, *Journal of Water and Environmental Nanotechnology*, **2(2)**: 129–135 (2017).

[32] Shojaei S., Ahmadi J., Davoodabadi Farahani M., Mehdizadehd B., Pirkamali M., Removal of Crystal Violet Using Nanozeolite-X From Aqueous Solution: Central Composite Design Optimization Study, *Journal of Water and Environmental Nanotechnology*, **4(1)**: 40–47 (2019).

[33] Shojaei S., Shojaei S., Experimental Design and Modeling of Removal of Acid Green 25 Dye by Nanoscale Zero-Valent Iron, *Euro-Mediterranean Journal for Environmental Integration*, **2(1)**: 15 (2017).

[34] Maamoun I., Eljamal O., Khalil A.M.E., Sugihara Y., Matsunaga, N., Phosphate Removal Through Nano-Zero-Valent Iron Permeable Reactive Barrier; Column Experiment and Reactive Solute Transport Modelling, *Transport in Porous Media*, **125(2)**: 395–412 (2018).

[35] Goleij M., Fakhraee H., Response Surface Methodology Optimization of Cobalt (II) and Lead (II) Removal from Aqueous Solution Using MWCNT-Fe_3O_4 nanocomposite, *Iranian Journal of Chemistry and Chemical Engineering (IJCCE)*, **36(5)**: 129–141 (2017).

[36] Navaei Diva T., Zare K., Taleshi F., Yousefi M., Removal of Cd^{2+} from Aqueous Solution by Nickel Oxide/CNT Nanocomposites, *Iranian Journal of Chemistry and Chemical Engineering (IJCCE)*, **38(1)**:141–154 (2019).

[37] Mehr H.V., Saffari J., Mohammadi S.Z., Shojaei S., The Removal of Methyl Violet 2B Dye Using Palm Kernel Activated Carbon: Thermodynamic and Kinetics Model, *International Journal of Environmental Science and Technology*, 1-10 (2019).

[38] Hameed B.H., Equilibrium and Kinetic Studies of Methyl Violet Sorption by Agricultural Waste, *Journal of Hazardous Materials*, **154(1)**: 204–212 (2008).

[39] Ho Y.S., Chiang T.H., Hsueh Y.M., Removal of Basic Dye from Aqueous Solution Using Tree Fern as a Biosorbent, *Process Biochemistry*, **40(1)**: 119–124 (2005).

[40] Sanchooli Moghaddam M., Rahdar S., Taghavi M., Cadmium Removal from Aqueous Solutions Using Saxaul Tree Ash, *Iranian Journal of Chemistry and Chemical Engineering (IJCCE)*, **35(3)**:45–52 (2016).

[41] Mubarak N.M., Sahu J.N., Abdullah E.C., Synthesis of Novel Magnetic Biochar Using Microwave Heating for Removal of Arsenic from Waste Water, *Iranian Journal of Chemistry and Chemical Engineering (IJCCE)*, **37(5)**:111–115 (2018).

[42] Visa, M., Duta, A., TiO_2/Fly Ash Novel Substrate for Simultaneous Removal of Heavy Metals and Surfactants, *Chemical Engineering Journal*, **223**: 860–868 (2013).

[43] Okte, A., Karamanis, D., Tuncel, D., Dual Functionality of TiO_2-Flyash Nanocomposites: Water Vapor Adsorption and Photocatalysis, *Catalysis Today*, **230**: 205–213 (2014).

[44] Yang, L., Wang, F., Hakki, A., Macphee, D.E., Liu, P., Hu, S., The influence of Zeolites Fly Ash Bead/TiO_2 Composite Material Surface Morphologies on their Adsorption and Photocatalytic Performance, *Applied Surface Science*, **392**: 687–696 (2017).

[45] Joshi, M.K., Pant, H.R., Liao, N., Kim, J.H., Kim, H.J., Park, C.H., Kim, C.S., In-Situ Deposition of Silver−Iron Oxide Nanoparticles on the Surface of Fly Ash for Water Purification, *Journal of Colloid and Interface Science*, **453**: 159–168 (2015).

[46] Karanac, M., Đolić, M., Veličković, Z., Kapidžić, A., Ivanovski, V., Mitrić, M., Marinković, A., Efficient Multistep Arsenate Removal onto Magnetite Modified Fly Ash, *Journal of Environmental Management*, **224**: 263–276 (2018).

[47] Chirkst D.E., Lobacheva O.L., Berlinskii I.V., Sulimova M.A., Recovery and Separation of Ce^{3+} and Y^{3+} Ions from Aqueous Solutions By Ion Flotation, *Russian Journal of Applied Chemistry*, **82(8)**: 1370−1374 (2009).

[48] Chirkst D.E., Lobacheva O.L., Dzhevaga N.V., Ion Flotation of Rare-Earth Metals with Sodium Dodecyl Sulfate, *Russian Journal of Applied Chemistry*, **84**: 1424−1430 (2011).

[49] Chirkst D.E., Lobacheva O.L., Dzhevaga N.V., Ion Flotation of Lanthanum(III) And Holmium(III) from Nitrate and Nitrate-Chloride Media, *Russian Journal of Applied Chemistry*, **85(1)**: 25−28 (2012).

[50] Saitoh T., Saitoh M., Hattori C., Hiraide M., Rapid Removal of Cationic Dyes from Water by Coprecipitation with Aluminum Hydroxide and Sodium Dodecyl Sulfate, *Journal of Environmental Chemical Engineering*, **2(1)**: 752−758 (2014).

[51] Jafari M., Abdollahzadeh A.A., Aghababaei F., Copper Ion Recovery from Mine Water by Ion Flotation, *Mine Water and the Environment*, **36(2)**: 323−327 (2017).

[52] Yang H.S., Han K.H., Kang D.W., Kim, Y.H., Removal of Metal Ions by Ultrafiltration of a Micellar Solution Containing Anionic Surfactant, *Korean Journal of Chemical Engineering*, **13(5)**: 448−452 (1996).

[53] Park S.J., Yoon H.H., Song S.K., Solubilization and Micellarenhanced Ultrafiltration of *o*-cresol by Sodium Dodecyl Sulfate Micelles, *Korean Journal of Chemical Engineering*, **14(4)**: 233−240 (1997).

[54] Ramenskaya L.M., Kraeva O.V., Dissociation Constants for the Zinc(II)-8-hydroxyquinoline Complexes in Aqueous and Sodium Dodecyl Sulfate Micellar Solutions, *Russian Journal of Physical Chemistry*, **80(1)**: 90-94 (2006).

[55] Mungray A.A., Kulkarni S.V., Mungray A.K., Removal of Heavy Metals from Wastewater Using Micellar Enhanced Ultrafiltration Technique: AReview, *Central European Journal of Chemistry*, **10(1)**: 27−46 (2012).

[56] Zhou H., Han G., Fu D., Chang Y., Xiao Y., Zhai H-J., Petal-Shaped poly(3,4-ethylenedioxythiophene)/Sodium Dodecyl Sulfate-Graphene Oxide Intercalation Composites for High-Performance Electrochemical Energy Storage, *Journal of Power Sources*, **272**: 203−210 (2014).

[57] Shawabkeh R.A., Abu-Nameh E.S.M., Absorption of Phenol and Methylene Blue by Activated Carbon from Pecan Shells, *Colloid Journal*, **69(3)**: 355−359 (2007).

[58] Ivanets M.G., Savitskaya T.A., Nevar T.N., Grinshpan D.D., Adsorptive and Structural Characteristics of Carbon Sorbents, *Inorganic Materials*, **47**: 1170−1175 (2011).

[59] Song X-I., Zhang M-W., Zhang Y., Huang S-T., Geng B-Y., Meng R-B., et al., Surface Modification of Coconut-Based Activated Carbon by SDS and Its Effects on Pb^{2+} Adsorption, *Journal of Central South University*, **20**(5): 1156−1160 (2013).

[60] Totur D., Bozkurt S.S., Merdivan M., Use of Pyrocatechol Violet Modified Sodium Dodecyl Sulfate Coated on Alumina for Separation and Preconcentration of Uranium(VI), *Journal of Radioanalytical and Nuclear Chemistry*, **292(1)**: 321−327 (2012).

[61] Mohammed R., El-Maghrabi H.H., Younes A.A., Farag A.B., Mikhail S., Riad M., SDS-Goethite Adsorbent Material Preparation, Structural Characterization and the Kinetics of the Manganese Adsorption, *Journal of Molecular Liquids*, **231**: 499−508 (2017).

[62] Reeve P.J., Fallowfield H.W., Natural and Surfactant Modified Zeolites: A Review of Their Applications for Water Remediation with a Focus on Surfactant Desorption and Toxicity Towards Microorganisms, *Journal of Environmental Management*, **205**: 253-261 (2018).

[63] Naushad M., Alothman Z.A., Alam M.M., Awual M.R., Eldesoky G.E., Islam M., Synthesis of Sodium Dodecyl Sulfate-Supported Nanocomposite Cation Exchanger: Removal and Recovery of Cu2+ from Synthetic, Pharmaceutical and Alloy Samples, *Journal of the Iranian Chemical Society*, **12(9)**: 1677-1686 (2015).

[64] Sobhanardakani S., Ahmadi M., Zandipak R., Efficient Removal of Cu(II) and Pb(II) Heavy Mmetal Ions from Water Samples Using 2,4-dinitrophenylhydrazine Loaded Sodium Dodecyl Sulfate-Coated Magnetite Nanoparticles, *Journal of Water Supply: Research and Technology*, **65**: 361−372 (2016).

[65] Sobhanardakani S., Zandipak R., 2,4-Dinitrophenylhydrazine Functionalized Sodium Sodecyl Sulfate-Coated Magnetite Nanoparticles for Effective Removal of Cd(II) and Ni(II) Ions from Water Samples, *Environmental Monitoring and Assessment*, **187**: 1−14 (2015).

[66] Montgomery D.C., "Design and Analysis of Experiments", John Wiley & Sons, New York (2008).

[67] Mori S., Hara T., Aso K., Okamoto H., Zeta Potential of Coal Fine-Particles in Aqueous Suspension, *Powder Technology*, **40(1−3)**: 161−165 (1984).

[68] Fuerstenau D.W., Rosenbaum J.M., You Y.S., Electrokinetic Behavior of Coal, *Energy Fuels*, **2(3)**: 241−245 (1988).

[69] Ghosh R.K., Reddy D.D., Tobacco Stem Ash as an Adsorbent for Removal of Methylene Blue from Aqueous Solution: Equilibrium, Kinetics, and Mechanism of Adsorption, *Water, Air, & Soil Pollution*, **224**: 1−12 (2013).

[70] Liu H.L., Chiou Y.R., Optimal Decolorization Efficiency of Reactive red 239 by UV/TiO2 Photocatalytic ProcessCoupled with Response Surface Methodology, *Chemical Engineering Journal*, **112(1−3)**: 173–179 (2005).

[71] Yuan X.Z., Meng Y.T., Zeng G.M., Fang Y.Y., Shi J.G., Evaluation of Tea-Derived Biosurfactant on Removing Heavy Metal Ions from Dilute Wastewater by ion Flotation, *Colloids and Surfaces A: Physicochemical and Engineering Aspects*, **317(1−3)**: 256−261 (2008).

[72] Aljeboree A.M., Alshirifi A.N., Alkaim A.F., Kinetics and Equilibrium Study for the Adsorption of Textile Dyes on Coconut Shell Activated Carbon, *Arabian Journal of Chemistry*, **10(2)**: S3381–S3393 (2017).

[73] El Nemr A., Potential of Pomegranate Husk Carbon for Cr(VI) Removal from Wastewater: Kinetic and Isotherm Studies, *Journal of Hazardous Material*, **161(1)**: 132−141 (2009).

[74] Sreejalekshmi K.G., Anoopkrishnan K., Anirudhan T.S., Adsorption of Pb(II) and Pb(II)-Citric Acid on Sawdust Activated Carbon: Kinetic and Equilibrium Isotherm Studies, *Journal of Hazardous Material*, **161(2−3)**: 1506−1513 (2009).

[75] Jalayeri H., Salarirad M.M., Ziaii M., Kinetics and Isotherm Modeling of Zn(II) Ions Adsorption onto Mine Soils, *Physicochemical Problems of Mineral Processing*, **52(2)**: 767−779 (2016).

[76] Irannajad M., Haghighi H.K., Soleimanipour M., Adsorption of Zn^{2+}, Cd^{2+} and Cu^{2+} on Zeolites Coated by Manganese and Iron Oxides, *Physicochemical Problems of Mineral Processing*, **52(2)**: 894−908 (2016).